Mixing efficiency in a run-down gravity current

G. O. Hughes[1] and P. F. Linden[2]

[1]Department of Civil and Environmental Engineering,
Imperial College London
g.hughes@imperial.ac.uk
[2]Department of Applied Mathematics and Theoretical Physics,
University of Cambridge
p.f.linden@damtp.cam.ac.uk

Abstract

We present measurements of mixing efficiency in a run-down gravity current created by lock exchange in a channel. Experiments were designed to extend to particularly high Reynolds number (of order 10^5, based on the current depth), at which mixing is no longer affected significantly by viscosity. Under these conditions, we observe that the run-down density profiles in the channel achieve full self-similarity and that the mixing efficiency asymptotes to a value of 0.08.

1 Introduction

Intense turbulence is a ubiquitous feature in gravity currents, but its dynamical importance is not well understood. Most previous studies have concentrated on understanding the bulk characteristics of currents such as the speed of propagation and current depth, highlighting the existence of a number of flow regimes and dynamical balances (e.g. see Huppert and Simpson, 1980; Rottman and Simpson, 1983; Shin et al., 2004; Simpson, 1997, for an overview). Measurements have revealed rich density and velocity structure in a turbulent gravity current (e.g. Hacker et al., 1996; Hallworth et al., 1996; Kneller et al., 1999; Shin et al., 2004; Marino et al., 2005; Fragoso et al., 2013; Samasiri and Woods, 2015; Sher and Woods, 2015). Interestingly, although turbulent eddies exchange mass and momentum between the current and ambient fluid, resulting in additional drag on the current and mixing of the density field, the propagation speed and the effective current depth is usually still well-predicted by an energy-conserving theory (for instance, see Shin et al., 2004). Consequently, most previous theoretical models for gravity currents also assume a highly idealized form based on lateral and/or depth averaging. 'Box' models are a common example of this approach (e.g. Huppert and Simpson, 1980), representing a two-dimensional current as a constant area rectangle that elongates along the boundary with time. Density and velocity structure in the current is not accounted for explicitly, these distributions instead being characterized as uniform. Even though bulk idealizations capture some dynamics associated with mixing (because the total buoyancy anomaly in the flow is conserved; Huppert, 2006), the internal structure of the current and its role in the overall flow remains a barely examined question.

In this paper, we examine the energy budget of the flow with the aim of generating insight into the dynamics governing turbulent mixing in a gravity current. We restrict attention here to conceptually simple laboratory experiments examining lock exchange currents in the constant speed regime (Rottman and Simpson, 1983), where we expect turbulent mixing to also proceed at an approximately constant rate. We report measurements of the mixing for Reynolds number $Re = UH/2\nu$ ranging up to 70,000, where U is the current

speed, $H/2$ is the current depth and ν is the kinematic viscosity. Thus, our approach seeks to measure the efficiency of mixing in a gravity current in a regime unaffected by viscosity. A limited number of previous studies have attained Reynolds numbers of a similar order to the current study, these having focused on different characteristics of the current (e.g. propagation speed and current height; Keulegan, 1958; Shin et al., 2004; Marino et al., 2005; Adduce et al., 2012) or on a time-dependent mixing regime (Fragoso et al., 2013; Sher and Woods, 2015). We describe the laboratory experiments in §2, the results in §3 and our conclusions in §4.

2 Experiments

2.1 Method

Six lock exchange experiments were conducted in a rectangular channel of length $L = 9.6\,\mathrm{m}$, width $0.25\,\mathrm{m}$ and depth $0.5\,\mathrm{m}$ (figure 1). A thin barrier was placed approximately half-way along the channel, i.e. $L_{\mathrm{lock}} = 4.8 \pm 0.1\,\mathrm{m}$, and one partition was filled with salt solution of density ρ_{H}. The rest of the channel was filled with fresh water (density ρ_{L}). The only parameter that was varied was the initial density difference ($\rho_{\mathrm{H}} - \rho_{\mathrm{L}}$) (table 1). The nominal depth of the fluid was $0.4 \pm 0.01\,\mathrm{m}$, but the initial free surface heights (H_{L} and H_{H}) were adjusted such that the pressures on each side of the barrier were equalized at approximately mid-depth (the values of H_{L} and H_{H} ranged from $0.402\,\mathrm{m}$ and $0.398\,\mathrm{m}$, respectively, at the smallest density difference, to $0.438\,\mathrm{m}$ and $0.376\,\mathrm{m}$ at the largest density difference).

Each experiment was started by removing the barrier vertically. A dense gravity current travels along the bottom of the channel (figure 2) and a light current travels in the opposite direction along the free surface. The currents reach and reflect from the far end walls, and the subsequent motions decay gradually under the action of viscosity. The tank was left to stand for at least a couple of hours to reach an equilibrated state with no motion.

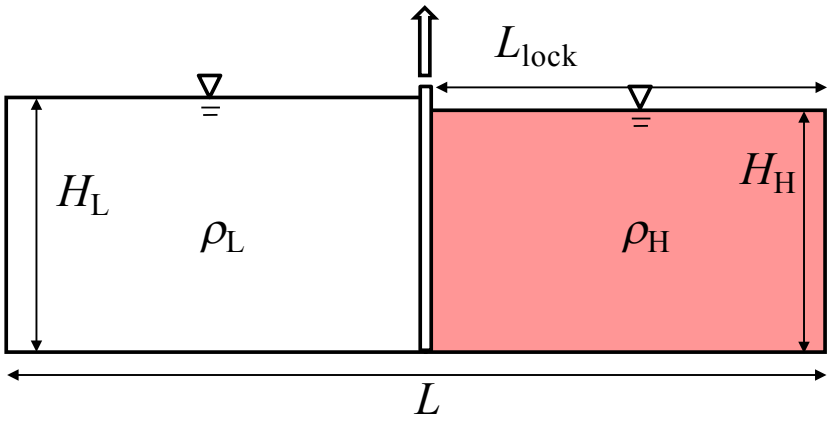

Figure 1: Schematic of the lock release experiment. Salty water of density ρ_{H} fills a lock of length L_{lock}, and fresher water of density ρ_{L} fills the remainder of the channel. The depth $H_{\mathrm{L}} > H_{\mathrm{H}}$ and is set so that the pressures on the two sides of the lock gate are the same at mid-depth of the channel. The barrier was removed vertically to begin the experiment.

Table 1: Summary of experiments: values of the dimensionless density difference $(\rho_{\mathrm{H}} - \rho_{\mathrm{L}})/\rho_0$, the speed of gravity current propagation U measured along the bottom and the Reynolds number $Re \equiv UH/2\nu$. The reference density ρ_0 is taken to be the average of ρ_{L} and ρ_{H}, and the uncertainty in U is based on the finite time taken to withdraw the barrier at the start of the experiment.

Experiment	$(\boldsymbol{\rho_{\mathrm{H}} - \rho_{\mathrm{L}})/\rho_0}$	$\boldsymbol{U}$ **m s^{-1}**	$\boldsymbol{Re}$
1	0.171	0.350±0.013	70,000
2	0.086	0.273±0.008	54,600
3	0.043	0.189±0.004	37,800
4	0.012	0.101±0.001	20,200
5	0.002	0.037±0.0002	7,400
6	0.172	0.360±0.013	72,000

Measurements were made of the densities and depths on both sides of the barrier initially and of the vertical density profile and total depth H at the end of the experiment. Great care was needed to measure the change in free surface height, which was determined to within 0.1 mm using a micrometer. The density profile at the end of the experiment was measured by withdrawing samples at predetermined depths. All density samples were measured with an Anton Paar densitometer, accurate to $10^{-3}\,\mathrm{kg\,m^{-3}}$. The range of density differences resulted in gravity current speeds $0.037 < U < 0.360\ \mathrm{m\,s^{-1}}$ along the tank base (current speeds along the free surface were marginally faster), with Reynolds numbers $Re \equiv UH/2\nu$ between 7,400 and 72,000.

Figure 2: Visualization of the gravity current with $Re = 72,000$ (Experiment 6; table 1). The current is dyed with food colouring and viewed against a translucent lined sheet.

2.2 Energy budget

Measurements of the density field before and after the experiment allow calculation of the energy used to irreversibly mix the fluid. For simplicity, we neglect non-Boussinesq effects in the following treatment of the energy budget. In the initial and final states (denoted by subscript i and f, respectively), where there is no motion, the total energy of the system is simply the potential energy,

$$PE_k = \int_{V_k} g\rho_k z dV_k, \quad k \in [i, f, nm], \tag{1}$$

where V_k, ρ_k and z are the fluid volume, density and vertical position of a fluid parcel, respectively, in the state k and g is the gravitational acceleration. We also introduce a third state – denoted by subscript "nm" – that would result if the density field in the initial state was adiabatically rearranged to a state of equilibrium (i.e. allowed to flow without any mixing taking place). This state is calculated theoretically from the initial state using conservation of volume.

The maximum potential energy that can be released in this flow is the available potential energy $PE_i - PE_{nm}$, and the energy consumed by irreversible mixing is $PE_f - PE_{nm}$. Thus the mixing efficiency $\mathcal{M}$ is defined as

$$\mathcal{M} \equiv \frac{PE_f - PE_{nm}}{PE_i - PE_{nm}}. \tag{2}$$

Note that if the mixing is complete so that the final density is uniform throughout the channel, the final potential energy PE_f approaches PE_i and $\mathcal{M} = 1$ in the limit where the initial differential of free surface height across the barrier vanishes.

3 Results

The flow structure shown in figure 2 is typical of all experiments. Large scale billows and intense turbulence are observed on the interface between the counter-flowing currents extending for several current depths behind each head. However, the intensity of the turbulence along the interface was noticeably reduced for the current with the lowest Reynolds number (Experiment 5, $Re = 7,400$). Qualitative observations indicate that turbulence is predominant during the gravity current phase of the flow, consistent with recent observations by Sher and Woods (2015) and Cenedese et al. (pers. comm.). Accordingly we assume that our results characterize the mixing associated with the gravity current phase. As is usual for a full-depth lock release, the current occupies about half the depth of the channel and initially travels at a constant speed. In the present experiments, this constant speed persists to the end of the channel because the channel length $L \ll 10L_{\text{lock}}$, which is the distance at which a gravity current enters the similarity phase and begins to decelerate (Rottman and Simpson, 1983). Hence we also anticipate the rate of mixing to be approximately constant throughout each experiment.

Figure 3 shows the final density profiles after all motion in the channel has ceased. The profiles are approximately self-similar when normalized by the initial density difference, with a final interfacial region that is symmetrical about mid-depth (defined as $z' = 0$) and significant mixing evident in the region $-0.2 \lesssim z'/H \lesssim 0.2$. A weak departure from this self-similar form is suggested at the two lowest Reynolds numbers (Experiments 4 and 5) by a larger density gradient at the centre of the interface. Despite fairly large density differences in Experiments 1 and 6 (the maximum $(\rho_{\text{H}} - \rho_{\text{L}})/\rho_0 \sim 0.17$), the symmetry about $z' = 0$ implies that non-Boussinesq effects are small (in keeping with only minor differences expected for density ratios $\rho_{\text{L}}/\rho_{\text{H}} > 0.85$; Lowe et al., 2005; Birman et al., 2005).

The results are consistent with a physical picture of the initiation, development and subsequent saturation of shear instability with distance behind each gravity current head. We would expect turbulent mixing at a given location to therefore be associated with the passage of the gravity current and the mixing to be suppressed once the instability has run its course and left behind a stabilized interfacial structure in its wake. The dimensionless interface thickness r (based on the maximum density gradient and normalised by the total depth) is equivalent to the gradient Richardson number Ri_g that evolves across the interface between the two currents. Indeed, $r \approx 0.33$ (figure 3) is consistent with previous studies of shear instability that have observed establishment of a stable interfacial region following a mixing event ($Ri_g \sim 0.3$, Thorpe, 1973; Smyth and Moum, 2000).

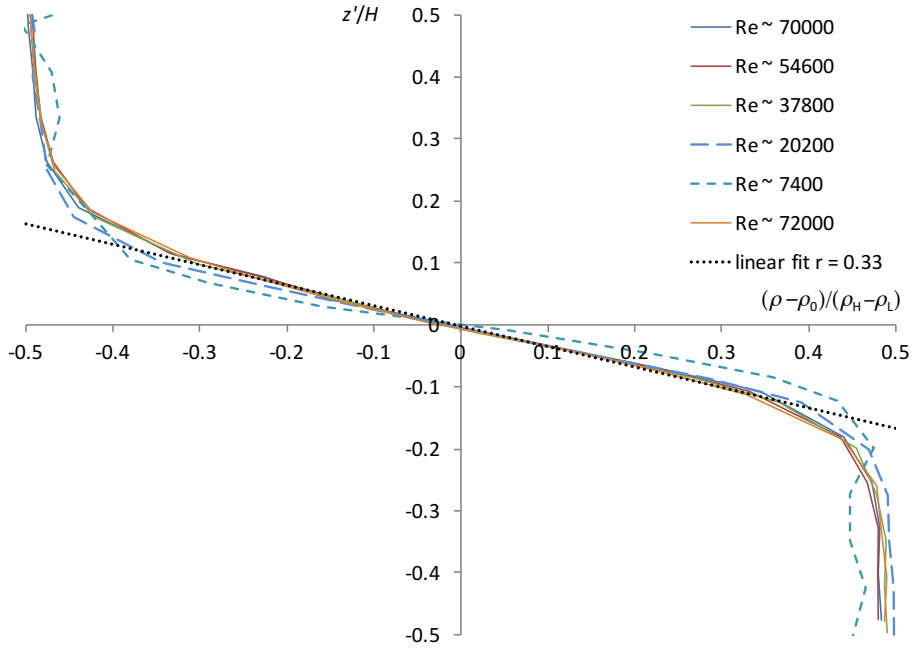

Figure 3: Final density profiles for the experiments in table 1 normalized by the initial density difference. The profiles were measured by withdrawing samples at different depths and the profiles are drawn with linear segments between the data points. Also shown is the linear density profile corresponding to an interfacial region with dimensionless thickness $r = 0.33$.

The mixing efficiency determined from the initial and final density fields is shown in figure 4. The values range from 0.05 to 0.08, and suggest a slight increase with Re to an asymptote at high Re. Unfortunately, we were unable to reach higher Re values with our laboratory facilities and so the asymptotic value cannot be confirmed. However, the value of approximately 0.08 agrees well with theoretical estimates (to be presented elsewhere).

4 Conclusions

The conceptually simple experiments presented here yield a range of insights into mixing caused by a gravity current. The qualitative observations and measurements are consistent with development of stratified shear instability associated with the passage of the gravity current head. At sufficiently high Reynolds number (of $O(30,000)$ based on the current depth), we find that the resulting density profile becomes self-similar; the thickness of the stabilized interface normalized by the total flow depth is close to a third. Interestingly, the interfacial signatures resulting from fully-developed Kelvin-Helmholtz instability and mixing are essentially identical (Thorpe, 1973; Corcos and Sherman, 1976; Koop and Browand, 1979; Smyth and Moum, 2000). This supports the notion that the ensuing turbulence and mixing in the lock exchange flow redistributes momentum and density in the vertical until the interface between the gravity currents is stabilized against further shear instability.

We find that up to about 0.08 of the energy supplied to the flow is consumed by irreversible mixing. At first glance, this value represents a mixing efficiency that is small compared to values of 0.15–0.2 that are thought to characterize the mixing owing to shear instability. However, it is important to recognise that these efficiencies measure physically different quantities. In this study we include in the energy budget the amount required

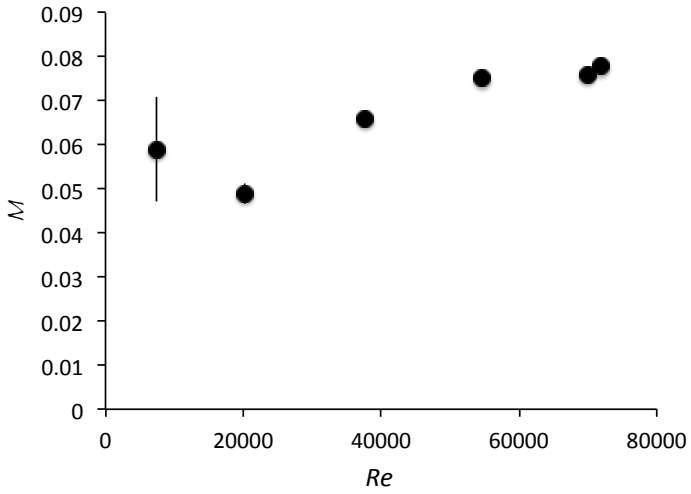

Figure 4: Mixing efficiency results plotted as a function of the Reynolds number Re. Error bars are calculated for each experiment and are determined mainly by the relative accuracy with which the changes in free surface height $H_{\mathrm{L}} - H$ and $H_{\mathrm{H}} - H$ can be measured. Note that the error bars exceed the symbol size only for the lowest two Re experiments.

to sustain the mean flow (i.e. the gravity currents), whereas a variety of measures are instead based on the proportion of energy supplied to turbulence that is consumed by mixing. Furthermore, these measures may rely on some form of averaging (e.g. in a volume, temporal or ensemble sense) or may be applicable at a specific position in the flow. Given that the turbulence in a lock-exchange gravity current is neither homogeneous nor statistically steady, we have chosen to characterize the flow by a bulk mixing efficiency measure that is unambiguous. The results highlight the importance of this consideration in a situation where the mean flow is integral to the location and characteristics of the turbulent mixing.

Finally, we have shown that the mixing associated with a gravity current only attains a self-similar asymptotic state at Reynolds numbers in excess of about 50,000 – well above the range typically thought to be necessary or considered in previous studies.

Acknowledgements

The authors gratefully acknowledge the skills and expertise provided by the technical staff of the G. K. Batchelor laboratory. This work was supported, in part, by the EPSRC Programme Grant EP/K034529/1.

References

Adduce, C., Sciortino, G., and Proietti, S. (2012). Gravity currents produced by lock exchanges: Experiments and simulations with a two-layer shallow-water model with entrainment. *J. Hydraul. Eng.*, 138:111–121.

Birman, V., Martin, J., and Meiburg, E. (2005). The non-boussinesq lock exchange problem. part 2. high resolution simulations. *J. Fluid Mech.*, 537:125–144.

Corcos, G. and Sherman, F. (1976). Vorticity concentration and the dynamics of unstable free shear layers. *J. Fluid Mech.*, 73:241–264.

Fragoso, A. T., Patterson, M. D., and Wettlaufer, J. S. (2013). Mixing in gravity currents. *J. Fluid Mech.*, 734:R2, doi:10.1017/jfm.2013.475.

Hacker, J., Linden, P. F., and Dalziel, S. B. (1996). Mixing in lock-release gravity currents. *Dyn. Atmos. Oceans*, 24:183–195.

Hallworth, M. A., Phillips, J., Huppert, H. E., and Sparks, R. S. J. (1996). Entrainment into two-dimensional and axisymmetric turbulent gravity currents. *J. Fluid Mech.*, 308:289–312.

Huppert, H. E. (2006). Gravity currents: a personal perspective. *J. Fluid Mech.*, 554:299–322.

Huppert, H. E. and Simpson, J. E. (1980). The slumping of gravity currents. *J. Fluid Mech.*, 99:785–799.

Keulegan, G. H. (1958). The motion of saline fronts in still water. *Natl Bur. Stnd. Rep.*, 5813.

Kneller, B., Bennett, S. J., and McCaffrey, W. D. (1999). Velocity structure, turbulence and fluid stresses in experimental gravity currents. *J. Geophys. Res.*, 104:5281–5291.

Koop, C. G. and Browand, F. (1979). Instability and turbulence in a stratified fluid with shear. *J. Fluid Mech.*, 93:135–159.

Lowe, R., Rottman, J., and Linden, P. (2005). The non-Boussinesq lock exchange problem. Part 1. Theory and experiments. *J. Fluid Mech.*, 537:101–124.

Marino, B. M., Thomas, L. P., and Linden, P. F. (2005). The front condition for gravity currents. *J. Fluid Mech.*, 536:49–78.

Rottman, J. W. and Simpson, J. E. (1983). Gravity currents produced by instantaneous releases of a heavy fluid in a rectangular channel. *J. Fluid Mech.*, 135:95–110.

Samasiri, P. and Woods, A. W. (2015). Mixing in axisymmetric gravity currents. *J. Fluid Mech.*, 782:R1, doi:10.1017/jfm.2015.519.

Sher, D. and Woods, A. W. (2015). Gravity currents: entrainment, stratification and self-similarity. *J. Fluid Mech.*, 784:130–162.

Shin, J. O., Dalziel, S. B., and Linden, P. F. (2004). Gravity currents produced by lock exchange. *J. Fluid Mech.*, 521:1–34.

Simpson, J. (1997). *Gravity currents in the environent and the laboratory.* Cambridge University Press.

Smyth, W. and Moum, J. (2000). Length scales of turbulence in stably stratified mixing layers. *Phys. Fluids.*, 12:1327–1342.

Thorpe, S. (1973). Experiments on instability and turbulence in a stratified shear flow. *J. Fluid Mech.*, 61:731–751.